Experimental Study on the Separability of Reaction-Deactivation Kinetics: Thermal Desorption of Alcohols from Fresh and Na-poisoned γ–Al_2O_3

Temperature programmed desorption (TPD) of methanol and ethanol from fresh and Na-poisoned γ–Al_2O_3 has been employed to investigate experimentally the separability of reaction-deactivation kinetics. The analysis of the TPD spectra has provided both an energetic characterization of the nonhomogeneous catalytic surface and the kinetic parameters of the desorption reaction, and has allowed quantitative discussion of the separability of the expression for the rate of desorption. The results obtained have been related to the chemical causes of nonseparability of reaction-deactivation kinetics; they also demonstrate the influence of catalyst decay on selectivity. For the systems considered, it appears that the assumption of separable deactivation kinetics is generally not a satisfactory approximation.

PIO FORZATTI,
MASSIMO BORGHESI,
ITALO PASQUON,
and ENRICO TRONCONI
Dipartimento di Chimica Industriale
ed Ingegneria Chimica del
Politecnico
Piazza Leonardo da Vinci, 32
I-20133 Milan, Italy

SCOPE

A common approach to reaction-deactivation kinetics results in a "separable" rate expression, written as $r = r_o(C_i,T)a$, where r_o is the rate on the fresh catalyst, while a is a multiplicative factor scaled between 0 and 1 accounting for the effects of catalyst decay.

The feasibility of a separable treatment of reaction-deactivation kinetics is addressed experimentally in this work by considering temperature programmed desorption (TPD) of methanol and ethanol from fresh and Na-poisoned γ-Al_2O_3, and assuming the desorption reaction as the model reaction. This seems a profitable approach, because TPD curve analysis is able in principle to provide a complete energetic and kinetic description of the reacting system, which is required to evaluate overall desorption rates in their separable and nonseparable forms, $(r_T)_S$ and $(r_T)_{NS}$. Thus it becomes possible to investigate both qualitatively and quantitatively, in terms of the ratio $(r_T)_{NS}/(r_T)_S$, the effects induced by poisoning on the kinetic description of the thermal desorption reaction for methanol and ethanol. This represents the objective of the present work. Since desorption of ethanol from γ-Al_2O_3 is known to result in the evolution of ethanol as well as ethylene, the TPD approach also allows an analysis of the effect of poisoning on selectivity.

CONCLUSIONS AND SIGNIFICANCE

The question of how to model deactivation kinetics has been experimentally investigated. For TPD of methanol and ethanol from Na-poisoned γ-Al_2O_3 a separable rate expression for the rate of desorption is generally incorrect because of the occurrence of a selective form of poisoning. Besides, changes in selectivity occur independently of any assumption on the separability of reaction-deactivation kinetics, so that they cannot be taken as conclusive evidence of nonseparability. It appears also that the separable representation provides a systematic overestimation of activity. These results have been related to their chemical causes, and are expected to apply as well to other reacting systems exhibiting similar chemical behavior. Finally, TPD has proven to be a suitable technique for studying the separability of reaction-deactivation kinetics.

Correspondence concerning this paper should be addressed to Pio Forzatti.

INTRODUCTION

The kinetic analysis of catalyst deactivation phenomena has commonly been grounded on the assumption that the deactivation rate may be separated from the rate of the main reaction (Szepe and Levenspiel, 1971). This approach has typically been applied to the study of deactivation by coking (Weekman, 1968; Wojchiechowski, 1974; Froment, 1980). A variety of reactions, such as dehydration, dehydrogenation, chlorination and cracking reactions, on catalysts including zeolites, silica-alumina, chromia, and supported metals, have been considered, separable deactivation models always providing a satisfactory description of the kinetics investigated. It has been noticed, however, that inconsistencies associated with the form of the deactivation model may not be apparent due to the parameterization required by the very complex reaction kinetics and chemical reactor models adopted (Butt et al., 1978). Nonetheless, a separable approach might be expected to be consistent with a mechanism of catalyst decay due to a purely physical coverage of active sites, as the coking process may be regarded to a first approximation. Actually, deactivation by coking may sometimes be a remarkably more complex process (Forzatti et al., 1981). Along these lines Ballivet et al. (1974) have explained the deactivation behavior of Si/Al catalysts with different Al content during cis-2-butene isomerization in terms of a preferential fouling of Lewis active sites with respect to Brönsted sites. On the other hand, separability of deactivation kinetics has led to difficulties when chemical poisoning is the mechanism of decay. Bakshi and Gavalas (1975) have investigated the dehydration of methanol and ethanol over Si/Al catalysts poisoned by *n*-butylamine. They have reported the following as specific effects of nonseparable kinetics:

a. The ratio $r(C,i)/r(C,j)$, where i,j represent two different poisoning states, varies as much as 40% over the concentration range investigated.

b. The selectivity (ethylene formation/ethanol consumption) increases twofold upon poisoning by butylamine.

c. Ether and ethanol formation rates change by about 10 to 30% each upon flow reversal in a reactor with a poison gradient.

d. The estimates for the constants appearing in their empirical rate expression vary significantly with the poison level.

Indeed, point (b) does not seem to be a proof of nonseparable kinetics, as discussed later in this paper. Point (d) is only an indirect proof of nonseparability and is not fully conclusive, since correlation between kinetic parameters is likely to occur (Forzatti and Buzzi-Ferraris, 1982). Therefore any speculation about the values of single parameters may be misleading in principle. However, the work by Bakshi and Gavalas seems to point to a situation where substantial deviations from separability occur; point (a) above is particularly significant. Weng et al. (1975) also experienced difficulties with the separable approach in interpreting the effect of thiophene poisoning on the kinetics of benzene hydrogenation over supported Ni. Later, Onal and Butt (1981) reported that the estimated adsorption equilibrium constants in the denominator of a Langmuir-Hinshelwood rate expression varied substantially with the amount of poison, thus providing an indication similar to that presented by Bakshi and Gavalas [point (d)]. Corado et al. (1975) showed spectroscopic evidence that deactivation by self-poisoning of γ-Al_2O_3 in the isomerization of 2,3-dimethyl-1-butene leads to a change in the reaction mechanism. Further evidence of nonseparable deactivation kinetics can be found in the area of structure-sensitive poisoning. Barbier (1980) has shown a dependence of deactivation upon crystallite size for the poisoning of benzene hydrogenation over Pt/Al_2O_3 by NH_3, while this reaction on Pt has been reported to be structure-insensitive.

Butt et al. (1978) have suggested a theoretical approach for dealing quantitatively with the problem of separability. Nonideal, heterogeneous surfaces are energetically characterized assuming several different distribution patterns of the heat of chemisorption q, and a separable treatment is applied to each homogeneous subunit of the surface by introducing a local activity factor, a_q. The authors consider very simple kinetics for a classical isomerization reaction sequence. In all the cases examined, results are presented as the calculated ratio $(r_T)_{NS}/(r_T)_S$, where $(r_T)_{NS}$ is the overall, nonseparable reaction rate obtained by summing up the contributions from all subunits, while $(r_T)_S$ is the corresponding separable reaction rate based on an activity factor averaged with respect to the q distribution. Such a ratio is found to differ from unity over a wide range of surface parameters and operating conditions. The authors' conclusion is that the representation of deactivation kinetics over nonideal surfaces by a separable model is usually incorrect. The separable representation of poisoning kinetics is shown to be valid only for ideal surfaces in the Langmuir sense with a single, coverage-independent heat of chemisorption.

A method to test a reaction for obeying separable kinetics has been also proposed by Löwe (1980).

It was the goal of the present work to carry out an experimental study designed to gain fundamental insight into the separability of deactivation kinetics. Following the approach of Butt et al. (1978), catalytic nonideal surfaces should be considered. Furthermore, a complete kinetic and energetic description of the heterogeneous catalytic surface is necessary for this purpose. Recently, methods of analysis of temperature programmed desorption (TPD) curves from nonhomogeneous surfaces have become available in the literature. Such methods provide the distribution of the activation energy of desorption, E_d, as a function of the surface coverage θ along with the other kinetic parameters for the rate of the desorption reaction. Therefore, TPD techniques appear suitable to test quantitatively the separability of deactivation kinetics by comparing fresh and poisoned catalyst, if the thermal desorption reaction is regarded as the model reaction under investigation. On the basis of previous work (Bakshi and Gavalas, 1975), desorption of alcohols from γ-Al_2O_3 was chosen as the experimental reaction-catalyst system. Since a proper inorganic poison was required to prevent poison desorption, and a basic nature was necessary for the poisoning agent, the catalyst samples were impregnated by NaOH solutions. It was decided to study thermal desorption of both methanol and ethanol, as representative of two different situations. In fact, while in the former case only methanol evolution is observed, both ethanol and ethylene are desorbed in the latter, so that an analysis of the effect of poisoning on selectivity becomes possible.

THEORY

During TPD runs a sample of catalyst (typically a bed of catalyst particles) previously saturated with a volatile species is subjected to a programmed temperature rise, usually according to a linear heating schedule, under continuous flow of an inert gas. The desorbing molecules are carried to a detector whose response is recorded continuously during the experiment. In the resulting TPD curve, the abscissa is associated with the temperature of the catalyst sample, whereas the ordinate is proportional to the gas-phase concentration of the desorbing species, C, in the well-mixed sample cell. Assuming that diffusional resistances and readsorption of the desorbing gas within the porous sample are negligible, the rate of the desorption reaction per unit volume of the isothermal catalyst is expressed for first-order kinetics as (Cvetanovic and Amenomyia, 1967)

$$r = v_m\left(-\frac{d\theta}{dt}\right) = v_m k_d \theta \qquad (1)$$

where the desorption rate constant, k_d, exhibits an Arrhenius-type temperature dependence,

$$k_d = A \exp(-E_d/RT) \quad (2)$$

For heterogeneous nonideal surfaces the desorption activation energy E_d is a function of surface coverage θ (Taylor and Weinberg, 1978).

The rate of desorption during TPD runs is conveniently evaluated from the overall mass balance at steady state on the desorbing species. Assuming differential conditions (Cvetanovic and Amenomyia, 1967),

$$Q\,C = V_s\,v_m\left(-\frac{d\theta}{dt}\right) \quad (3)$$

Based on Eqs. 1, 2, and 3, procedures are available for analyzing the TPD spectra in order to derive the distribution of the coverage-dependent activation energy of desorption, $E_d(\theta)$ (Taylor and Weinberg, 1978; Forzatti et al., 1984).

For the purpose of studying reaction-deactivation kinetics, we have applied an approach originally presented for an ideal reaction $(A \rightarrow B)$ (Butt et al., 1978) to the experimental kinetics of the thermal desorption reaction. Hence, Eq. 1 provides the rate expression for our model reaction, and the required energetic description of the nonideal catalytic surface is given by the $E_d(\theta)$ profile resulting from the analysis of TPD spectra. Then, each value of desorption energy, E_d, can be associated with a homogeneous subunit of the heterogeneous surface. For each subunit, the separable representation of deactivation kinetics is appropriate (Butt et al., 1978), therefore we can define a local activity factor $a_i(E_d)$, corresponding to a desorption energy E_d on a catalyst with a level of poison i,

$$a_i = \frac{r_i(E_d)}{r_o(E_d)} = \frac{v_{m,i}k_d(E_d)\theta_i(E_d)}{v_{m,o}k_d(E_d)\theta_o(E_d)} = \frac{v_{m,i}\theta_i}{v_{m,o}\theta_o} \quad (4)$$

An overall nonseparable rate of desorption is specified as

$$(r_T)_{NS,i} = \frac{\int_{E_{d1}}^{E_{d2}} a_i(E_d)r_o(E_d)dE_d}{E_{d2} - E_{d1}} \quad (5)$$

E_{d2} and E_{d1} being the upper and lower limits of the desorption energy distribution.

On the other hand, a separable form for the overall rate of desorption results from introducing an average activity,

$$\bar{a}_i = \frac{\int_{E_{d1}}^{E_{d2}} a_i(E_d)dE_d}{E_{d2} - E_{d1}} = \frac{v_{m,i}}{v_{m,o}(E_{d2} - E_{d1})}\int_{E_{d1}}^{E_{d2}}\frac{\theta_i}{\theta_o}dE_d \quad (6)$$

Then,

$$(r_T)_{S,i} = \frac{\bar{a}_i}{E_{d2} - E_{d1}}\int_{E_{d1}}^{E_{d2}} r_o(E_d)dE_d \quad (7)$$

A comparison between a separable and a nonseparable rate form can be presented in terms of the ratio

$$\frac{(r_T)_{NS,i}}{(r_T)_{S,i}} = \frac{\int_{E_{d1}}^{E_{d2}} a_i r_o dE_d}{\bar{a}_i\int_{E_{d1}}^{E_{d2}} r_o dE_d} = \frac{\int_{E_{d1}}^{E_{d2}}\theta_i(E_d)\exp(-E_d/RT)dE_d}{\bar{a}_i\int_{E_{d1}}^{E_{d2}}\theta_o(E_d)\exp(-E_d/RT)dE_d} \quad (8)$$

Deviations of this ratio from unity imply that the separable and nonseparable rate forms are not consistent. Notice that evaluation of the integrals appearing in Eq. 8 requires knowledge of the $E_d(\theta)$ distribution of the nonideal surface, as obtained from the analysis of the TPD curves.

EXPERIMENTAL

The apparatus used for TPD experiments is schematically shown in Figure 1. Helium was used as the carrier gas, with a typical flow rate of 2.5 cm^3/s at STP conditions. During a few runs the flow rate was systematically

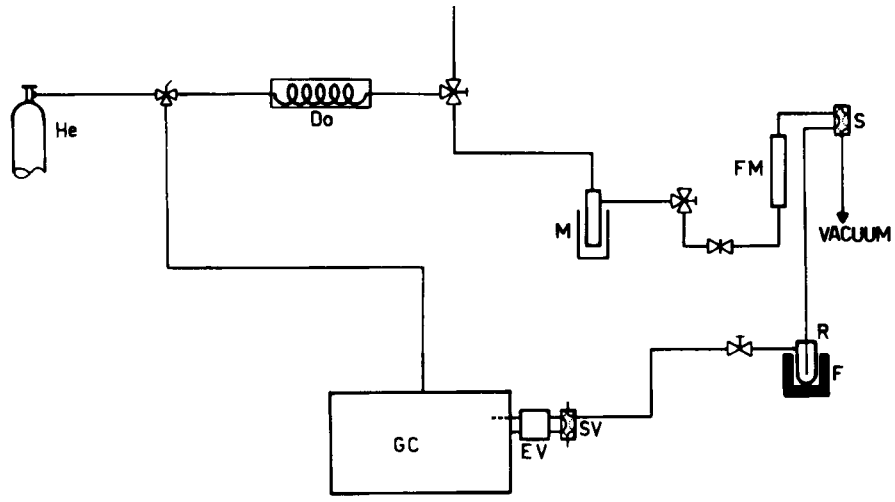

Figure 1. Schematic diagram of the TPD apparatus.

DO, deoxo unit	**F, furnace**
M, molecular sieve column	**SV, sampling valve**
FM, flowmeter	**GC, gas chromatograph**
S, six-way valve	**EV, eight-way valve**
R, reactor	

Table 1. Catalyst Parameters and TPD Operating Conditions for Methanol and Ethanol Desorption from Fresh and Na-poisoned γ-Al_2O_3

Catalyst Parameters	
Average particle radius, R_p	3.7×10^{-3}cm
Porosity	0.56
Surface area, α_s	3.4×10^{6} cm^2/g
TPD Operating Conditions	
Catalyst load, W_c	0.05 g
Catalyst volume, V_s	6.7×10^{-2} cm^3
Geometric surface area, $S = 3V_s/R_p$	54 cm^2
Carrier gas flow rate, Q	2.5 cm^3/s
Heating rate, β	0.17 K/s
Est. effective diffusivity, D_e (Knudsen)	
CH_3OH (T = 380 K)	1.0×10^{-2} cm^2/s
C_2H_5OH (T = 398K)	0.9×10^{-2} cm^2/s

decreased down to 0.5 cm^3/s in order to determine the significance of readsorption, as discussed in the following. Helium from a cylinder was passed through a Cu deoxo unit at 463 K and through a molecular sieve cooled with liquid nitrogen to remove traces of oxygen and water, respectively. A reactor design similar to that described by Cvetanovic and Amenomyia (1967) was adopted in order to ensure fully homogeneous conditions in the catalyst bed. The temperature of the catalyst bed was raised according to a linear heating schedule by use of a Perkin Elmer programming controller, the heating rate β being 0.17 K/s during all runs. The temperature was measured by means of an iron-constantan thermocouple directly immersed in the catalyst bed. All tubes and connections after the reactor were heated to prevent condensation of the desorbed species. The quartz reactor, containing 0.05 g of catalyst, was connected directly to a flame ionization detector from a Carlo Erba 2350 Fractovap gas chromatograph (GC) with no separation column inserted in the line. Thus, the concentration of the desorbed species in the carrier gas stream was continuously monitored, from which TPD spectra were obtained.

Each TPD run was started with a fresh catalyst sample. A commercial γ-Al_2O_3 (Ketijen Grade B) was used. The relevant catalyst parameters are listed in Table 1. The procedure reported by Pines and Haag (1960) was followed to prepare the poisoned catalyst. γ-Al_2O_3 was impregnated with a solution of NaOH, the volume of water being equal to the volume of pores (1.8 cm^3/g). Two levels of poison were considered, the amount of Na added being 0.8 and 1.5 wt. % for levels 1 and 2, respectively. The samples in the form of powder (200–230 mesh) were dried in air for two hours, and then pretreated *in situ* at 773 K in flowing He for two hours, in order to remove physisorbed water. Cooling to room temperature followed under flow of He. This procedure was designed in order to prevent dehydration of the catalyst surface during TPD runs, where a maximum temperature of about 723 K was reached.

Then, a few pulses of alcohol were passed over the catalyst bed at room temperature until saturation was achieved. The reactor, still at room temperature, was then evacuated at 1.3×10^{-3} bar (0.13×10^{-3} MPa) for 10 min to remove the weakly physisorbed gases. A few experiments performed at higher partial pressure of the adsorbate in the pulses and with different vacuum conditions during the pretreatment confirmed that the initial coverage was always equal to unity. After adsorption and evacuation the carrier gas was allowed to flow over the catalyst bed for 30 min, then the TPD run was begun and the TPD trace recorded. After completion of the run, each TPD experiment was repeated with a fresh catalyst sample. In this case the carrier gas line was modified so as to bypass the GC, and samples of the carrier gas containing the desorbed species were periodically analyzed using a gas sampling valve and a Porapak T separation column 1 m long (80–120 mesh) included in the GC and operated isothermally at 423 K. Thus, the nature of the desorbing species could be checked.

Reproducibility of TPD experiments was found satisfactory, based on replicated runs. Chromatographic helium, and methanol and ethanol Merck RP reagents were used druing all runs. An experiment with smaller catalyst particle size (300-320 mesh) was also performed in order to determine whether diffusional limitations were present.

RESULTS AND DISCUSSION

Methanol Desorption

TPD Spectra. Table 1 summarizes typical experimental conditions for methanol desorption from fresh γ-Al_2O_3. The thermal desorption spectra of methanol from fresh and Na-poisoned γ-Al_2O_3 are shown in Figure 2. The gas chromatographic analysis of

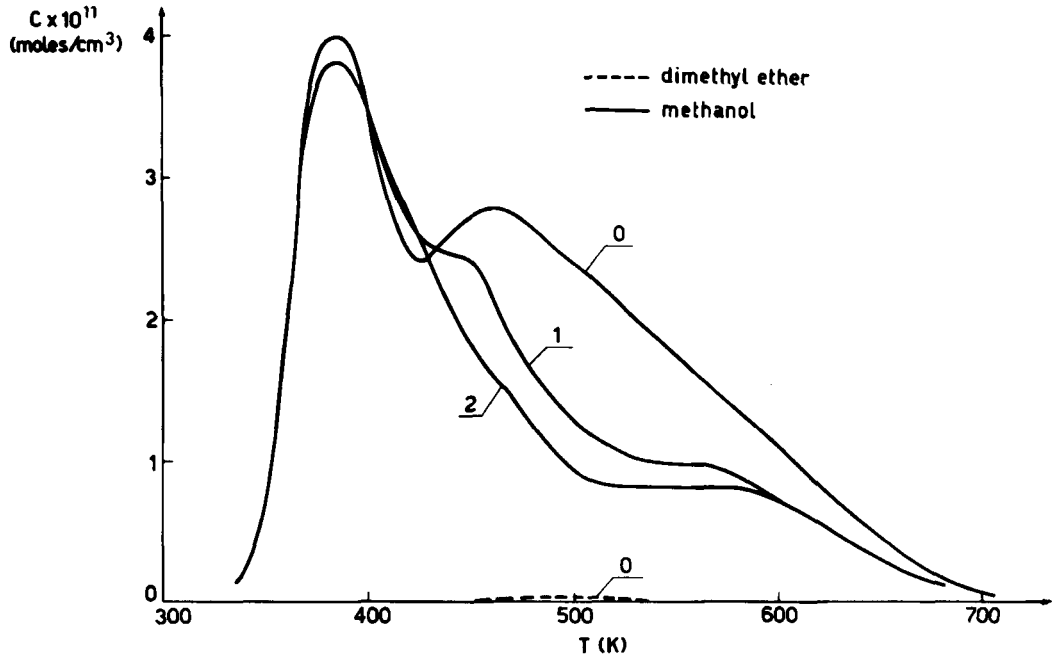

Figure 2. Thermal desorption curves of methanol from γ-Al_2O_3. Poison level 0 = 0% Na; level 1 = 0.8% Na; level 2 = 1.5% Na.

the desorbed species confirmed that the curves represent methanol desorption only, other compounds such as formaldehyde and decomposition products being practically absent. Small amounts of dimethyl ether were observed in the temperature range 450–550 K, but could safely be neglected in the analysis. No carbon deposition was observed. The complex shape of the TPD curve with two peak maxima and peak asymmetry is related to the heterogeneity of the γ-Al_2O_3 surface with Brönsted and Lewis sites of different acidic strength. Actually, several investigators (Greenler, 1962; Deo and Dalla Lana, 1969; Deo et al., 1971; Hertl and Cuenca, 1973) have demonstrated by IR techniques that the adsorption of alcohols on γ-Al_2O_3 occurs through the interaction of the alcohol hydroxyl with either a surface hydroxyl or a Lewis site and an oxygen pair. This causes the formation of a liquidlike methanol species or a methoxy surface compound. The impregnation of γ-Al_2O_3 with NaOH solutions reduces the amount of methanol desorbed at temperatures above 420 K, which indicates a preferential poisoning of the active sites with higher activation energy. This agrees with the observation that NaOH impregnation causes a preferential poisoning of the more acidic Lewis and Brönsted sites (Peri, 1965; Deo et al., 1971).

A more detailed discussion of the chemistry of methanol desorption from γ-Al_2O_3 seems beyond the scope of the present work, where only an empirical description of the desorption kinetics has been sought. Excellent references on the subject are Knözinger and Ratnasamy (1978), and Scokart and Rouxet (1982).

Regime Analysis. The feasibility of a steady state treatment was confirmed by application of theoretical criteria (Gorte, 1982) that compare the average residence time of the desorbed species in the sample cell, and the time for the desorbed species to diffuse out of the sample, with the total experiment time.

The assumption of negligible mass transfer limitations was validated both by calculations and experimentally. Gorte's criterion III, which compares the time of intraparticle diffusion with the sample contact time, yields $QR_p/D_eS = 1.7 \times 10^{-2} \ll 0.1$. Refer to Table 1 for constants. Also, the TPD curves are unaffected by a 30% reduction in particle size. In particular, no shift in the peak temperature was recorded, whereas it has been demonstrated, both theoretically (Herz et al., 1982; Gorte, 1982) and experimentally (Tronconi and Forzatti, 1985) that the peak temperature depends on the size of the catalyst particle in a diffusion-controlled regime. On the basis of both verifications above, our conclusion is that information derived from TPD spectra is not disguised by diffusional effects.

To determine the significance of readsorption, both theoretical and experimental considerations were again invoked. We evaluated the dimensionless group $(\alpha_s W_c k_a/Q)$, representing the ratio of the readsorption rate to the net measured desorption rate. A crude estimate for the adsorption rate constant, $k_a = 8 \times 10^{-9}$ cm/s, was obtained from the amount of alcohol required to saturate the catalyst bed before the TPD run was started. Then, $\alpha_s W_c k_a/Q = 5.4 \times 10^{-4} \ll 0.1$.

An experimental criterion for the absence of readsorption was also devised, as follows. The general form of Eq. 1, including readsorption effects, is (Cvetanovic and Amenomyia, 1967)

$$v_m\left(-\frac{d\theta}{dt}\right) = v_m k_d \theta - \alpha_s \varrho_c k_a C(1-\theta) \qquad (9)$$

On introducing Eq. 9 into Eq. 3, and rearranging,

$$\frac{1}{C} = \frac{1}{V_s v_m k_d \theta} Q + \frac{\alpha_s \varrho_c k_a (1-\theta)}{V_s v_m k_d \theta} \qquad (10)$$

Suppose that a number of TPD spectra have been recorded corresponding to diverse gas rates, Q. If readsorption is not significant, plots of $1/C$ against Q at fixed T and θ values result in straight lines through the origin according to Eq. 10, the second term in the RHS being negligibly small. Figure 3 indicates that this is actually the case for our data.

As a consequence of the treatment presented in this section, Eqs. 1–3 may be correctly used for the analysis of our TPD curves.

Analysis of TPD Spectra. The kinetic analysis of the TPD curves for methanol desorption from fresh and Na-poisoned γ-Al_2O_3 was performed according to the procedure proposed by Forzatti et al. (1984). The results of the analysis are presented in Figure 4 as plots of desorption activation energy E_d against surface coverage θ for the three levels of poison considered. The value of $E_d(\theta)$ ranges approximately between 70 and 115 J/mol in all cases, whereas the three curves mostly diverge in the range $0.2 < \theta < 0.85$ owing to the existence of nonuniform poisoning.

Separability of Deactivation Kinetics. In Figures 5 and 6 we present calculated values for the ratio $(r_T)_{NS}/(r_T)_S$ in the case of poison levels 1 and 2, respectively. Equation 8 was used to compute this ratio from the $E_d(\theta)$ profiles of Figure 4. The effects of both temperature and initial surface coverage $\theta°$ are illustrated. Deviation of $(r_T)_{NS}/(r_T)_S$ from unity is significant for methanol desorption, and becomes more relevant for poison level 2, as the effect of selective poisoning is stronger in this case. The separable rate form

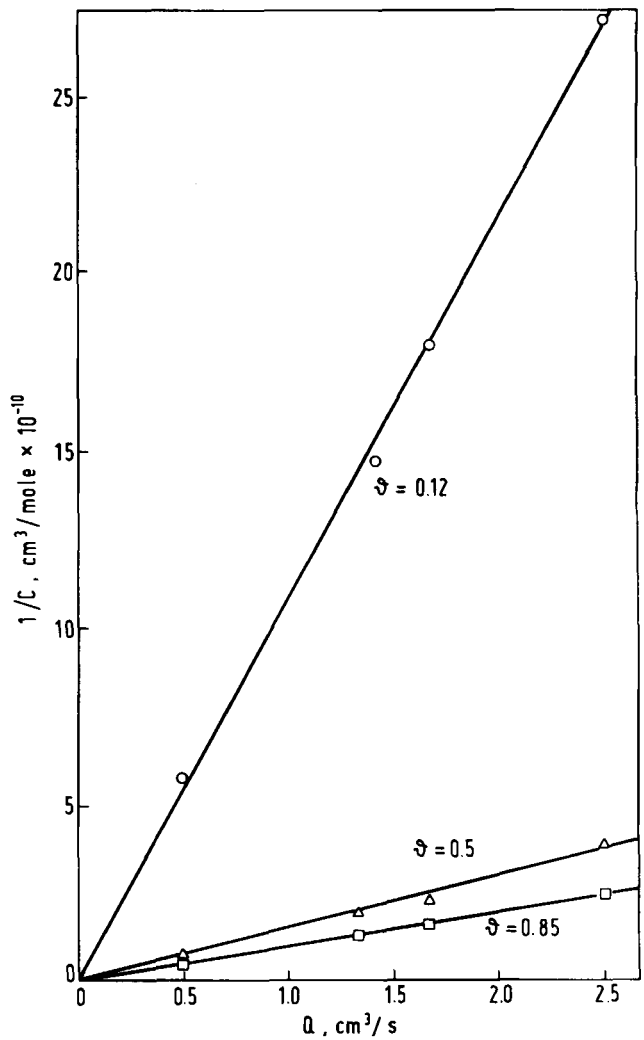

Figure 3. Methanol desorption from 1.5% Na-poisoned γ-Al_2O_3. Plot of $1/C$ vs. Q at different θ values for estimation of readsorption significance.

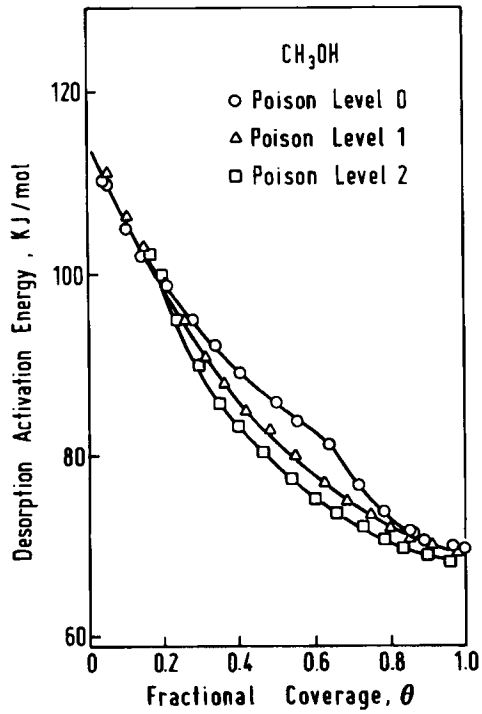

Figure 4. Calculated distribution profiles of activation energy for methanol desorption from fresh and Na-poisoned γ-Al_2O_3. Poison level 0 = 0% Na; level 1 = 0.8% Na; level 2 = 1.5% Na.

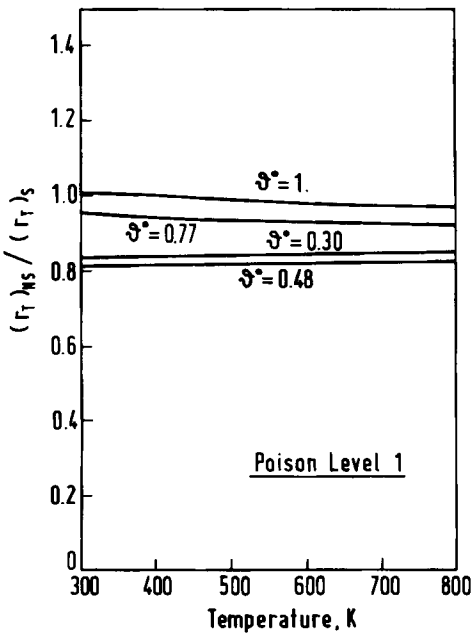

Figure 5. Methanol desorption from 0.8% Na-poisoned γ-Al_2O_3. Plots of calculated $(r_T)_{NS}/(r_T)_S$ vs. temperature, initial coverage θ° as a parameter.

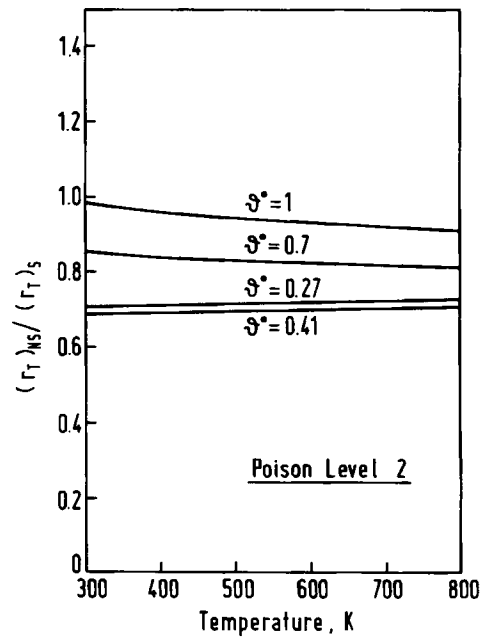

Figure 6. Methanol desorption from 1.5% Na-poisoned γ-Al_2O_3. Plots of calculated $(r_T)_{NS}/(r_T)_S$ vs. temperature, initial coverage θ° as a parameter.

appears to overestimate the rate of the desorption recation; this agrees with the fact that the most active sites are those preferentially poisoned. Accordingly, local activities corresponding to higher desorption energies are much smaller than the average activity (see Eq. 8). Temperature has a limited effect, in agreement with previous simulation results (Butt et al., 1978). In order to rationalize the effect of θ° it is worth considering that initial coverages corresponding to the region where the gap between the energy profiles is wider emphasize the effect of nonuniform poisoning, so that an approximate separable rate form becomes less acceptable, and stronger deviations of $(r_T)_{NS}/(r_T)_S$ from unity are expected. For very small initial coverages, however, Figure 4 shows that it becomes more and more difficult to distinguish between the poisoned and unpoisoned samples. Therefore, $(r_T)_{NS}/(r_T)_S$ tends to a limiting value of one as θ° approaches zero.

Ethanol Desorption

TPD Spectra. In Table 1 we give typical experimental conditions for ethanol desorption from fresh and poisoned γ-Al_2O_3. The thermal desorption curves of ethanol for levels of poison 0 and 2 are shown in Figure 7. On the basis of gas chromatographic analysis of the desorbed species, each curve can be resolved basically into two components associated with ethanol and ethylene evolution, respectively. Small amounts of diethyl ether were detected in the temperature range 450–550 K, but were neglected in this analysis. Also, no carbon deposition was observed. Two peaks are apparent in Figure 8 for ethanol desorption from fresh γ-Al_2O_3, with maxima at 398 and 490 K. When γ-Al_2O_3 is poisoned, the peak at 490 K almost disappears, the other peak being only reduced in size. Therefore, existence of preferential poisoning is confirmed as in the case of methanol desorption, but a uniform poisoning process seems to be superimposed on it. Again, the preferential poisoning applies to active sites with higher energy of activation.

Inspection of Figure 7 shows that Na acts as a poisoning agent as far as ethanol evolution is concerned, while it enhances the amount of ethylene desorbed and shifts the ethylene desorption

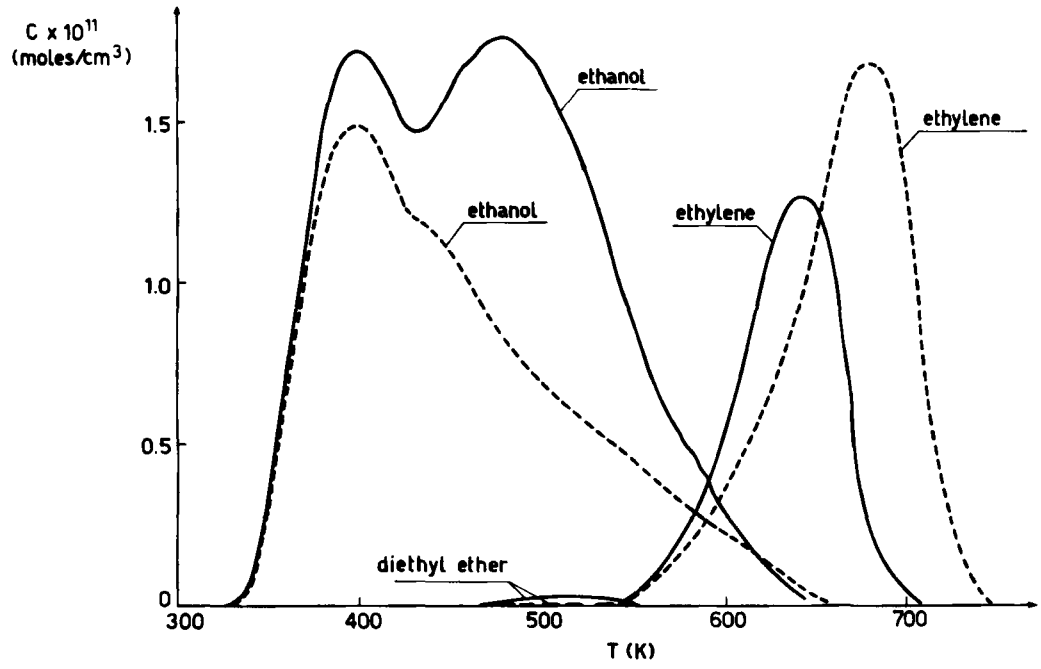

Figure 7. Thermal desorption curves of ethanol and ethylene from γ-Al_2O_3. ——— poison level 0 = 0% Na. - - - - - - poison level 2 = 1.5% Na.

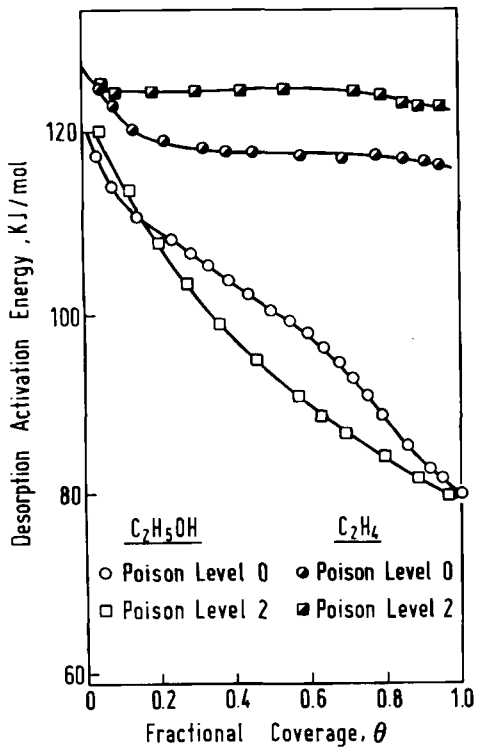

Figure 8. Calculated distribution profiles of activation energy for ethanol and ethylene desorption from fresh and Na-poisoned γ-Al_2O_3. Poison level 0 = 0% Na; level 2 = 1.5% Na.

peak to higher temperatures. The effect of Na poisoning on ethanol desorption resembles that already discussed for methanol desorption. As for ethylene evolution, the observed results seem to be consistent with a proposed mechanism of alkene formation, which implies that the β-hydrogen should be removed by interaction with a suitable basic site on the oxide surface (John and Scurrel, 1977; Pines and Manassen, 1966; Knözinger, 1976). If such an interaction does not occur in the adsorbed state, the alcohol is desorbed either unchanged or in the form of the corresponding ether, or as decomposition products. Actually, poisoning by Na results in transforming >Al-OH species into >Al-O-Na species (Deo and Dalla Lana, 1969). This accounts for a greater number of basic sites, as well as for a greater basicity of the new sites, so that both the greater amount of ethylene desorbed and the higher temperature of the desorption peak can be rationalized. This discussion illustrates the complexity of the poisoning process even for such a relatively simple reaction pattern of the general form $A \rightarrow B \rightarrow C$, as ethanol thermal desorption can be regarded. Particularly, the selectivity is surely altered in this case by the catalyst deactivation, but this result shows no direct relationship with the separability of the kinetics, contrary to what has been sometimes claimed in the literature.

Regime Analysis. When ethanol replaces methanol as the adsorbed species, no relevant change occurs among the parameters governing TPD. Hence, we have limited ourselves to check the absence of diffusional effects and readsorption by theoretical calculations. Refer to Table 1 for numerical values of the constants. Gorte's criterion III applied to ethanol desorption yields $QR_p/D_eS = 1.9 \times 10^{-2} \ll 0.1$, so that intraparticle concentration gradients appear negligible in this case too. As for readsorption, an estimated $k_a = 6 \times 10^{-9}$ cm/s yields $W_c a_s k_a/Q = 4.1 \times 10^{-4} \ll 0.1$. Again, readsorption is not significant.

Analysis of TPD Spectra. The kinetic analysis of the two component curves in Figure 7 was carried out separately by considering distinct characteristic rate parameters for the two desorption processes of ethanol and ethylene. The effect of poisoning on the distribution of desorption activation energies for both ethanol and ethylene desorption is presented in Figure 8. Ethylene de-

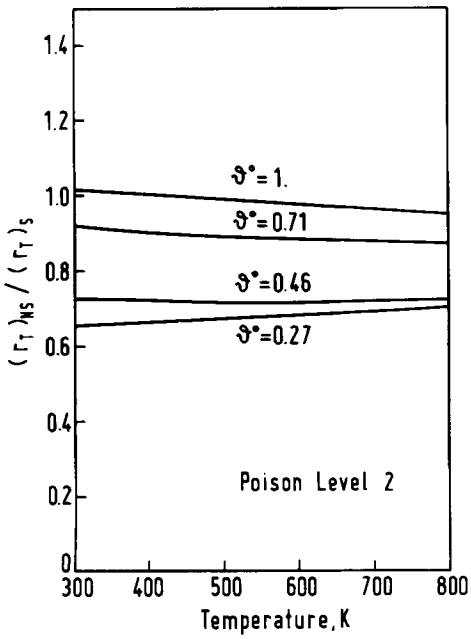

Figure 9. Ethanol desorption from 1.5% Na-poisoned γ-Al_2O_3. Plots of calculated $(r_T)_{NS}/(r_T)_S$ vs. temperature, initial coverage θ° as a parameter.

sorption is characterized by a roughly constant activation energy, corresponding to a peak shape for this product which closely resembles that from a homogeneous surface (see Figure 7). The increased E_d after poisoning is consistent with the higher temperature of the ethylene desorption peak. For ethanol desorption, calculated activation energies of the desorption reaction are in the range 80–120 J/mol, while nonuniform poisoning is manifest in the interval $0.2 < \theta < 0.8$.

Separability of Deactivation Kinetics. Figure 9 is a plot of the calculated ratio $(r_T)_{NS}/(r_T)_S$ for ethanol desorption only, the overall separable and nonseparable rate forms being defined as in the case of methanol desorption. The results are in fact similar. Only a small temperature effect is evident, while the initial surface coverage significantly affects the separability of the kinetics. The predictions of the separable rate form seem to exceed those obtained from the nonseparable form in this case too.

CONCLUSIONS

It is worth pointing out that temperature programmed desorption has proven to be a suitable experimental tool for investigating the separability of reaction-deactivation kinetics, as it is able in practice to provide a complete energetic and kinetic description of nonideal, heterogeneous catalytic surfaces, allowing for a direct study on the effect of poisoning processes upon the separability of the rate form.

The assumption of separability turned out to be critical for our examples of methanol and ethanol desorption from γ-Al_2O_3 because of the occurrence of a selective form of poisoning. Only for initial surface coverages close to one, when the preferentially poisoned sites are a relatively small fraction of the total number of catalytic sites, did a separable form of deactivation kinetics, although incorrect in principle, represent the phenomena to a good approximation. Besides, a uniform poisoning was found superimposed on a selective poisoning process for ethanol desorption. In such a case, separability of the kinetics depends on the relative weight of the two contributions, and in principle situations are possible where the choice between separable and nonseparable rate expressions becomes less critical. Also, the ratio $(r_T)_{NS}/(r_T)_S$ was found significantly less than one over a wide range of temperatures and initial coverages. It seems therefore that the separable rate form tends to provide a systematic overestimation of the catalyst activity as a result of an incorrect averaging process. In fact the strongest sites (high energy), which are those preferentially poisoned, exhibit lower local activities than the average activity appearing in the separable rate expression. Finally, the results of ethanol thermal desorption suggest that the poisoning process affects the selectivity of the reaction network independently of any assumption on the separability of deactivation kinetics. Na added to the catalyst acts as a poison as far as ethanol evolution is considered, but it also promotes the formation of more sites for ethylene desorption. Hence, changes in selectivity do not appear to provide conclusive evidence of nonseparable kinetics.

Although most of these conclusions strictly refer to the systems investigated, it was possible to achieve rationalization in terms of chemical evidence, so that it is reasonable to expect similar results when other reacting systems exhibiting similar chemical behavior are considered.

ACKNOWLEDGMENT

This work was supported by Italian Consiglio Nazionale delle Ricerche, Rome (Progetto Finalizzato "Chimica Fine e Secondaria".)

NOTATION

A = preexponential factor for the desorption rate constant, s^{-1}
a = activity factor in a separable rate expression
$a_i(E_d)$ = activity of a homogeneous surface subunit for the level of poison i
$\bar{a}_i$ = averaged activity for the level of poison i
C = concentration of the desorbed species in the carrier gas, mol/cm^3
D_e = effective diffusivity, cm^2/s
E_d = activation energy of the desorption reaction, kJ/mol
i,j = levels of catalyst poison
k_a = rate constant for adsorption, cm/s
k_d = rate constant for desorption, s^{-1}
q = heat of chemisorption, kJ/mol
Q = carrier gas flow rate, cm^3/s
R = gas constant, kJ/mol•K
R_p = particle radius, cm
r = rate of reaction, or rate of desorption, mol/cm^3•s
$(r_T)_{NS}, (r_T)_S$ = overall rate of reaction for nonseparable and separable kinetics, respectively, mol/cm^3•s
r_o = rate of reaction on fresh catalyst, mol/cm^3•s
S = external geometric area of the solid phase, cm^2
t = time, s
T = temperature, K
v_m = amount of volatile species adsorbed at saturation per catalyst unit volume, mol/cm^3
V_s = volume of the solid phase, cm^3
W_C = catalyst load, g

Greek Letters

α_s = catalyst active surface area, cm^2/g
β = heating rate, K/s
θ = fractional surface coverage

θ° = coverage of the desorbing surface at beginning of TPD run

θ_o, θ_i = fractional surface coverage at current temperature on fresh and poisoned (level i) catalyst, respectively

ϱ_c = catalyst density, g/cm^3

LITERATURE CITED

Bakshi, K.R., and G.R. Gavalas, "Effects of Nonseparable Kinetics in Alcohol Dehydrogenation over Poisoned Silica-Alumina," *AIChE J.* **21**, 494 (1975).

Ballivet, D., D. Barthoumeuf, and Y. Trambouze. "The Isomerization of cis-2-Butene over Silica Alumina Catalysts. III: Dependence on Alumina Content," *J. Catal.* **35**, 359 (1974).

Barbier, J., et al, "Selective Poisoning by Coke Formation on Pt/Al_2O_3," *Catalyst Deactivation*, B. Delmon and G.F. Froment, Eds., Elsevier, Amsterdam, 53 (1980).

Butt, J.B., C.K. Watcher, and R.M. Billimoria, "On the Separability of Catalytic Deactivation Kinetics," *Chem. Eng. Sci.*, **33**, 1,321 (1978).

Corado, A., et al., "Catalytic Isomerization of Olefins on Alumina. II: Catalyst Deactivation and Its Effects on the Mechanism," *J. Catal.*, **37**, 68 (1975).

Cvetanovic, R.J., and Y. Amenomiya, "Application of a Temperature Programmed Desorption Technique to Catalyst Studies," *Adv. Catal.*, **17**, 103 (1967).

Deo, A.V., and I.G. Dalla Lana, "An Infrared Study of the Adsorption and Mechanism of Surface Reaction of 1-Propanol on γ-Alumina and γ-Alumina Doped with Sodium Hydroxide and Chromium Oxide," *J. Phys. Chem.*, **73**, 716 (1969).

Deo, A.V., T.T. Chuang, and I.G. Dalla Lana, "Infrared Studies of Adsorption and Surface Reactions of Some Secondary Alcohols, C_3 to C_5, on γ-Alumina and γ-Alumina Doped with Sodium Hydroxide," *J. Phys. Chem.*, **75**, 234 (1971).

Forzatti, P., et al. "Disattivazione dei Catalizzatori. I: Aspetti Chimici e Cinetici," *Chim. Ind.*, Milan **63**, 575 (1981); *Int. Chem. Eng.* **24**, 60 (1984).

Forzatti, P., and G. Buzzi-Ferraris, "Reaction-Deactivation Kinetics of Methanol Oxidation Over a Silica Supported Fe_2O_3-MoO_3 Catalyst," *Ind. Eng. Chem. Proc. Des. Dev.*, **21**, 67 (1982).

Forzatti, P., et al., "Thermal Desorption from Heterogeneous Surfaces. Normalized Curve Treatment," *Surface Sci.*, **137**, 595 (1984).

Froment, G.F., "A Quantitative Approach to Catalyst Deactivation by Coke Formation," *Catalyst Deactivation*, B. Delmon, and G.F. Froment, Eds, Elsevier, Amsterdam, 1 (1980).

Gorte, R.J., "Design Parameters for Temperature Programmed Desorption from Porous Catalysts," *J. Catal.*, **75**, 164 (1982).

Greenler, R.G., "Infrared Study of the Adsorption of Methanol and Ethanol on Aluminium Oxide," *J. Chem. Phys.*, **17**, 2,094 (1962).

Hertl, W., and A.M. Cuenca, "Infrared Kinetic Study of Reactions of Alcohols on the Surface of Alumina," *J. Phys. Chem.*, **77**, 1,120 (1973).

Herz, R.K., J.B. Kiela, and S.P. Marin, "Adsorption Effects During Temperature Programmed Desorption of Carbon Monoxide from Supported Platinum," *J. Catal.*, **73**, 66 (1982).

John, C.S., and M.S. Scurrell, "Catalytic Properties of Aluminas for Reactions of Hydrocarbons and Alcohols," *Catalysis*, The Chemical Society, London, **I**, 136 (1977).

Knözinger, H., "Specific Poisoning and Characterization of Catalytically Active Oxide Surfaces," *Adv. Catal.*, **25**, 184 (1976).

Knözinger, H., and P. Ratnasamy, "Catalytic Aluminas: Surface Models and Characterization of Surface Sites," *Catal. Rev. Sci. Eng.*, **17**(1), 31 (1978).

Löwe, A., "Strategien Kinetischer Experimente mit Desaktivierenden Katalysatoren" (Strategies of Kinetics Experiments with Decaying Catalysts), *Chem.Ing.Technik*, **52**, 777 (1980).

Onal, I., and J.B. Butt, "Kinetic Separability of Catalyst Poisoning," *Stud. Surf. Sci. Catal.*, **7**, 1,490 (1981).

Peri, J.B., "A Model for the Surface of γ-Alumina," *J. Phys. Chem.*, **69**(1), 220 (1965).

Pines, H., and W.O. Haag, "Alumina: Catalyst and Support. I: Alumina, Its Intrinsic Acidity and Catalytic Activity," *J. Am. Chem. Soc.*, **82**, 2,471 (1960).

Pines, H., and J. Manassen, "The Mechanism of Dehydration of Alcohols Over Alumina Catalysts," *Adv. Catal.*, **16**, 49 (1966).

Scokart, P.O., and P.G. Rouxhet, "Comparison of the Acid-Base Properties of Various Oxides and Chemically Treated Oxides," *J. Colloid Interface Sci.*, **86**(1), 96 (1982).

Szepe, S., and O. Levenspiel, "Catalyst Deactivation," Proc. 4th Eur. Symp. Chem. React. Eng., Pergamon Press, Oxford, 265 (1971).

Taylor, J.L., and W.H. Weinberg, "A Method for Assessing the Coverage Dependence of Kinetic Parameters: Application to Carbon Monoxide Desorption from Iridium(110)," *Surface Sci.*, **78**, 259 (1978).

Tronconi, E., and P. Forzatti, "Experimental Criteria for Diffusional Limitations During TPD from Porous Catalysts," *J. Catal.*, **93**, 197 (1985).

Weekman, V.W., Jr., "A Model of Catalytic Cracking Conversion in Fixed, Moving, and Fluid-Bed Reactors," *Ind. Eng. Chem. Proc. Des. Dev*, 7, 90 (1968).

Weng, H.S., C. Eigenberger, and J.B. Butt, "Catalyst Poisoning and Fixed Bed Reactor Dynamics," *Chem. Eng. Sci.*, **30**, 1,341 (1975).

Wojchiechowski, B.W., "The Kinetic Foundations and the Practical Application of the Time on Stream Theory of Catalyst Decay," *Catal. Rev. Sci. Eng.*,**9**, 79 (1974).

Manuscript received Jan. 3, 1984, and revision received Feb. 28, 1985.